Electronic Supplementary Material (ESI) for ChemComm.

Supplementary Information

Computational Prediction of Hetero-Interpenetration in Metal-Organic Frameworks

Ohmin Kwon[a,*], Sanghoon Park[a,*], Hong-Cai Zhou[b], and Jihan Kim[a,**]

[a] Department of Chemical and Biomolecular Engineering, Korea Advanced Institute of Science and Technology, 291 Daehak-ro Yuseong-gu, Daejeon 305-338, Republic of Korea.

[b] Department of Chemistry, Texas A&M University, College Station, TX, 77843, USA.

.

[*]These authors contributed equally to this work.

[**]**Corresponding author email:** jihankim@kaist.ac.kr

S1 Algorithm to Identify Hetero-Interpenetrated Metal-Organic Frameworks

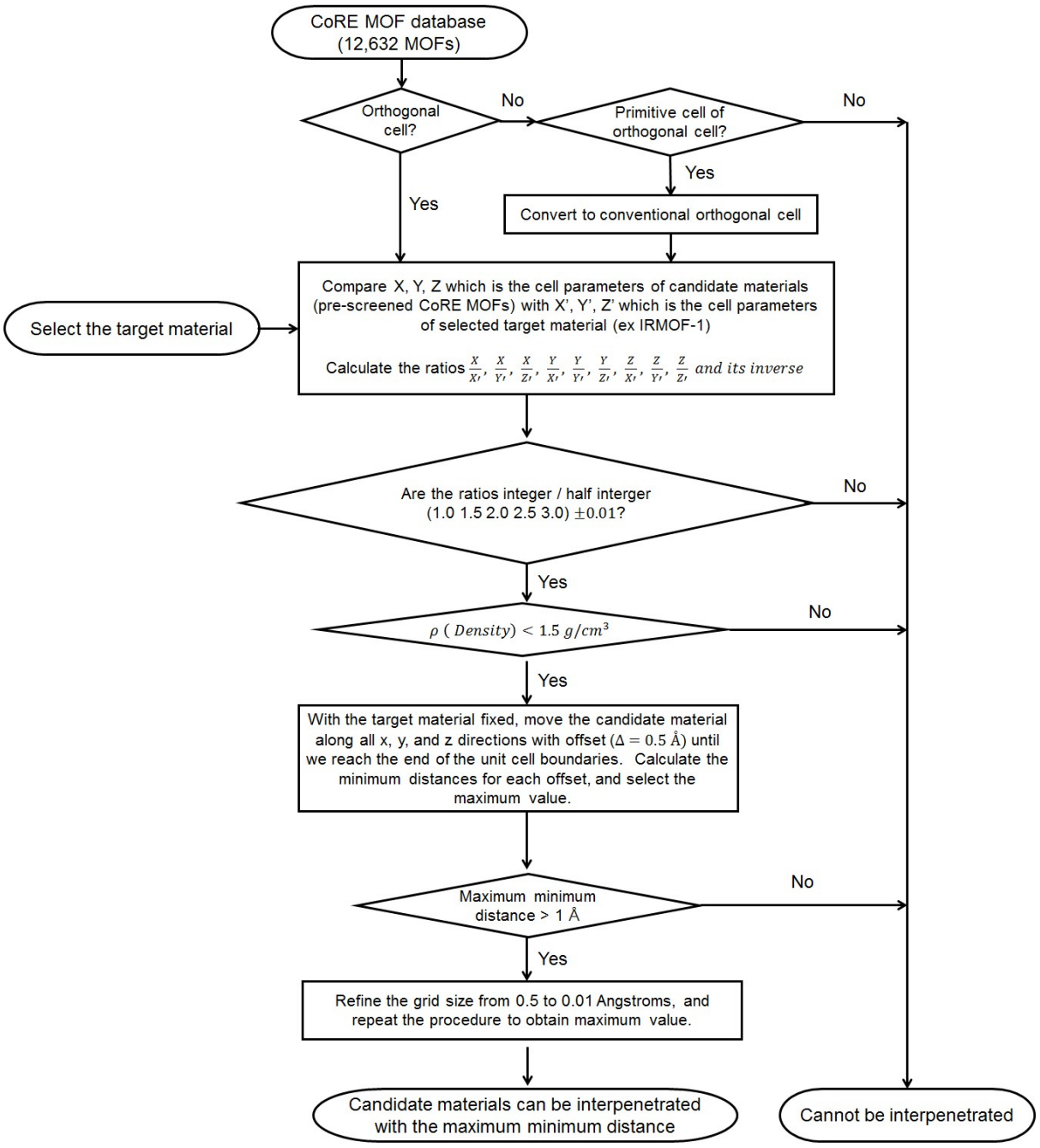

Figure S1: The flow chart of the algorithm used in this work.

S2 Summary of Hetero-interpenetrated MOF candidates for 300 Orthogonal Cell CoRE MOF Structures with Lowest Densities

Note: Some of these CCDC code MOFs that have different names might actually be the same structure, in which case few of these candidate matches might not be hetero-interpenetration, but homo-interpenetration. Also, we removed structures that have same CCDC six letter code but different numbers attached to them, that are essentially the same structure(s). For this screening, we only included structures with max min distance of 1.5 Angstroms or larger. The table is sorted in order from largest min distance to smallest. All structures except those marked by * have cubic cells.

Target MOF REFCODE	Cell Parameter of Target MOF (Angstrom)	Candidate MOF REFCODE	Cell Parameter of Candidate MOF (Angstrom)	Max_min length of interpenetrated structure (Angstrom)
VEBHUG	29.184	TEQPEM	29.171	4.71292
ZELROZ	17.1227	EDUVOO	34.381	4.466766
LAWGUM	25.898	COJTAX	25.7386	4.015631
COJTAX	25.7386	SAHYOQ	25.8849	4.014326
LAWGOG	25.889	COJTAX	25.7386	4.010536
PIBNUK01	25.6349	PIBNUK	25.6415	3.986011
COJTAX	25.7386	LAWGIA	25.872	3.983725
COJTAX	25.7386	LAWGEW	25.856	3.979077
COJTAX	25.7386	SAHYIK	25.669	3.978697
COJTAX	25.7386	EDUSIF	25.832	3.975131
COJTAX	25.7386	UNIGEE	25.6572	3.922847
BAZGAM	68.3112	SEMNIJ	68.706	3.827451
ZELROZ	17.1227	IZUSEC	17.16	3.754422
EDUVOO	34.381	IZUSEC	17.16	3.716019
SAHYOQ	25.8849	LAWGEW	25.856	3.616475
LAWGOG	25.889	UNIGEE	25.6572	3.577353
LAWGUM	25.898	EDUSIF	25.832	3.55786
EDUSIF	25.832	LAWGEW	25.856	3.557732
LAWGIA	25.872	EDUSIF	25.832	3.553284
LAWGUM	25.898	LAWGIA	25.872	3.54979
SAHYOQ	25.8849	LAWGIA	25.872	3.548406
LAWGUM	25.898	UNIGEE	25.6572	3.540682
UNIGEE	25.6572	SAHYOQ	25.8849	3.539022
LAWGOG	25.889	EDUSIF	25.832	3.538623
SAHYOQ	25.8849	EDUSIF	25.832	3.535649
UNIGEE	25.6572	LAWGEW	25.856	3.535518
SAHYOQ	25.8849	SAHYIK	25.669	3.535424
LAWGOG	25.889	SAHYIK	25.669	3.530998
LAWGUM	25.898	LAWGEW	25.856	3.530133

SAHYIK	25.669	LAWGEW	25.856	3.526972
UNIGEE	25.6572	LAWGIA	25.872	3.509768
LAWGIA	25.872	LAWGEW	25.856	3.498847
LAWGUM	25.898	SAHYOQ	25.8849	3.495087
LAWGOG	25.889	LAWGEW	25.856	3.494265
EDUSIF	25.832	SAHYIK	25.669	3.487769
SAHYIK	25.669	LAWGIA	25.872	3.486061
LAWGUM	25.898	SAHYIK	25.669	3.478496
LAWGOG	25.889	LAWGIA	25.872	3.474535
LAWGOG	25.889	SAHYOQ	25.8849	3.472457
LAWGUM	25.898	LAWGOG	25.889	3.471139
EDUSIF	25.832	UNIGEE	25.6572	3.464569
UNIGEE	25.6572	SAHYIK	25.669	3.428104
COJTAX	25.7386	XAMDUM	26.3368	3.34273
PUZLOM	37.461	MUWQEB	18.8235	3.243739
HEXVEM	49.6188	VETSUK	49.821	3.059971
HEXVEM	49.6188	VETTAR	49.744	2.987928
LUKLIN	37.23	UTEWOG	18.549	2.912832
ADATEG	68.604	BAZGAM	68.3112	2.909911
NIBJAK	52.993	HAFTOZ	26.4908	2.901383
RUTNOK	42.9245	VEJHEZ	43.03	2.882868
COJTAX	25.7386	AXUBAW	25.6135	2.861773
LURRIA	51.67	COJTAX	25.7386	2.84451
LUKLIN	37.23	VEXYON	18.595	2.827241
RUTNOK	42.9245	MUDTEL	42.833	2.754232
EWUHIO	27.26	EWUHOU	27.3	2.675444
RUTNOK	42.9245	VUJBIM	42.7958	2.656513
RUTNOK	42.9245	VUJBEI	42.8434	2.603252
HEXVEM	49.6188	VEGBUG	49.964	2.599642
PUZLOM	37.461	VEXYON	18.595	2.559757
VAZTOG	31.0569	LAFRER	64.412	2.527538
HEXVEM	49.6188	VEGCAN	49.84	2.508609
VAZTOG	31.0569	LAFROB	64.197	2.506441
EDUSIF	25.832	XAMDUM	26.3368	2.479008
LAWGUM	25.898	XAMDUM	26.3368	2.450417
SEMNEF	64.528	VAZTOG	31.0569	2.44994
LAWGIA	25.872	XAMDUM	26.3368	2.44949
LAWGEW	25.856	XAMDUM	26.3368	2.430442

SAHYOQ	25.8849	XAMDUM	26.3368	2.419364
LAWGOG	25.889	XAMDUM	26.3368	2.410246
PUZLOM	37.461	UTEWUM	18.807	2.304542
LAWGEW	25.856	AXUBAW	25.6135	2.265857
MUWQEB	18.8235	UTEWUM	18.807	2.249305
EDUSIF	25.832	AXUBAW	25.6135	2.240225
RUTNOK	42.9245	MUDTAH	42.854	2.227382
BAZFUF	27.4719	QOWRAV01	27.418	2.219923
SAHYIK	25.669	AXUBAW	25.6135	2.216136
UNIGEE	25.6572	AXUBAW	25.6135	2.212825
PUZLOM	37.461	UTEWOG	18.549	2.191093
HEXVEM	49.6188	BOXFOK	49.267	2.158822
NIBJAK	52.993	HABRAF	52.738	2.147221
UTEWOG	18.549	VEXYON	18.595	2.112925
PUZMAZ	74.972	PUZLOM	37.461	2.010445
XALTIP	30.995	ABEMIF	15.384	2.003581
UPOZAB	31.0569	ABEMIF	15.384	1.992191
RIFDUG01	26.54	DOTSOV	26.2833	1.990927
LURRIA	51.67	LAWGOG	25.889	1.970291
LURRIA	51.67	LAWGEW	25.856	1.962531
OXOLAP	39.845	OXOLET	39.8144	1.962471
NIBHOW	46.636	NAYZOE	23.211	1.956673
LURRIA	51.67	EDUSIF	25.832	1.953744
LURRIA	51.67	LAWGUM	25.898	1.953064
LURRIA	51.67	UNIGEE	25.6572	1.946808
RUTNOK	42.9245	RAHNOF	42.71	1.942091
LURRIA	51.67	LAWGIA	25.872	1.928537
LURRIA	51.67	SAHYOQ	25.8849	1.9093
XAMDUM	26.3368	DOTSOV	26.2833	1.908138
VEBHUG	29.184	BIWSEG	29.03	1.905229
TEQPEM	29.171	REGXOS	29.0302	1.90111
FIQCEN	26.343	DOTSOV	26.2833	1.898051
LURRIA	51.67	SAHYIK	25.669	1.864
OWITAQ	22.266	OWITEU	22.2434	1.848491
XALTIP	30.995	UPOZAB	31.0569	1.785686
ZELROZ	17.1227	XAMHEA*	17.1168 17.2215 17.2215	1.758925
HABRAF	52.738	DOTSOV	26.2833	1.7577

WEHHUO*	12.5059 26.1708 26.2509	DAKVOC*	12.4105 26.2172 26.2215	1.636332
ZELROZ	17.1227	EWIDUK	17.0357	1.61056
VEBHUG	29.184	REGXOS	29.0302	1.578539
WEHHUO*	12.5059 26.1708 26.2509	WEHHIC*	12.3830 26.2710 26.2780	1.566198
RUTNOK	42.9245	IGOCUD	21.6265	1.565987
WEHHOI*	12.3100 26.2500 26.3410	WEHHIC*	12.3830 26.2710 26.2780	1.56536
BAZGAM	68.3112	EDUVOO	34.381	1.56262
DAWMUL	63.515	ADASAB	63.931	1.549748
XALTIP	30.995	UVEVUN	31.105	1.521081

S3 Grand Canonical Monte Carlo Simulation

To compute the adsorption isotherm data, we used our in-house developed GPU-based code[1,2]. Given the parallel computing capacity of the GPU, multiple MC simulations can be performed simultaneously and resulting in significant amount of speedup compared to a typical CPU code. The GPU cards used for all of our simulations are from our own cluster: GeForce GTX TITAN Z and GeForce GTX 780. To accelerate computations further, energy grid with a spacing of 0.15 Å was generated as a lookup table for the simulations.

The interaction energies between gas molecule and framework atoms were modeled using a 12-6 Lennard-Jones (LJ) potential model (eq. 1) with a cut-off distance of 12.8 Å.

$$U_{LJ}(r) = 4\varepsilon\left[\left(\frac{\sigma}{r}\right)^{12} - \left(\frac{\sigma}{r}\right)^{6}\right] \qquad (1)$$

where U_{LJ} is the potential energy, ε is the well-depth, σ is the equilibrium distance, and r is the distance between interacting particles. The force-field parameters for framework atoms were taken from UFF[3]. For gas molecules, Buch Lennard-Jones potentials[4] (σ = 2.96 Å and ε = 34.2 K), and TraPPE force field[5] were utilized for H_2, and CH_4, respectively. To compute interaction energies between dissimilar atoms, the Lorentz-Berthelot mixing rules were adopted. In particular, the Feynman-Hibbs (FH) effective potential[6,7] was used to correct for the quantum effects that become more relevant from at low temperatures for hydrogen simulations (T = 77K). The quadratic approximation to the FH potential was used as it is known to be accurate enough to estimate the thermodynamic and dynamic properties[8,9].

$$U_{FH}(r) = V_{LJ}(r) + \left(\frac{\beta \hbar^2}{24\mu_m}\right)\left[\frac{d^2}{dr^2}V_{LJ}(r) + \frac{2}{r}\frac{d}{dr}V_{LJ}(r)\right] \quad (2)$$

$\beta = (k_B T)^{-1}$ where k_B is the Boltzmann constant and T is temperature, ħ is the reduced Planck's constant, and μ_m = m/2 is the educed mass of interacting pair of fluid.

S4 Experiment vs Simulated Adsorption Isotherm for H_2 and CH_4 in IRMOF-1, IRMOF-8, PCN-68, PCN-610

In order to verify the veracity of our GCMC results, we aggregated as much experimental data that we can find on the MOF structures relevant to our work. Subsequently, we compared out simulation data with the following available experimental data.

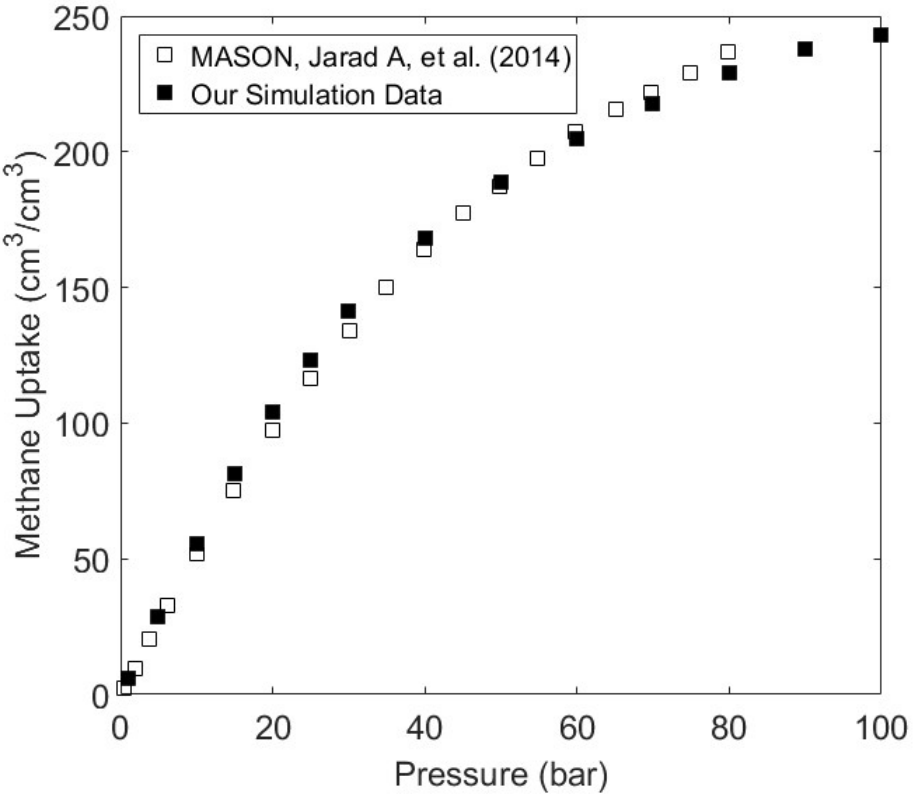

Figure S4-1: Experimental[10] vs simulated CH_4 adsorption isotherms in IRMOF-1 at T = 298K.

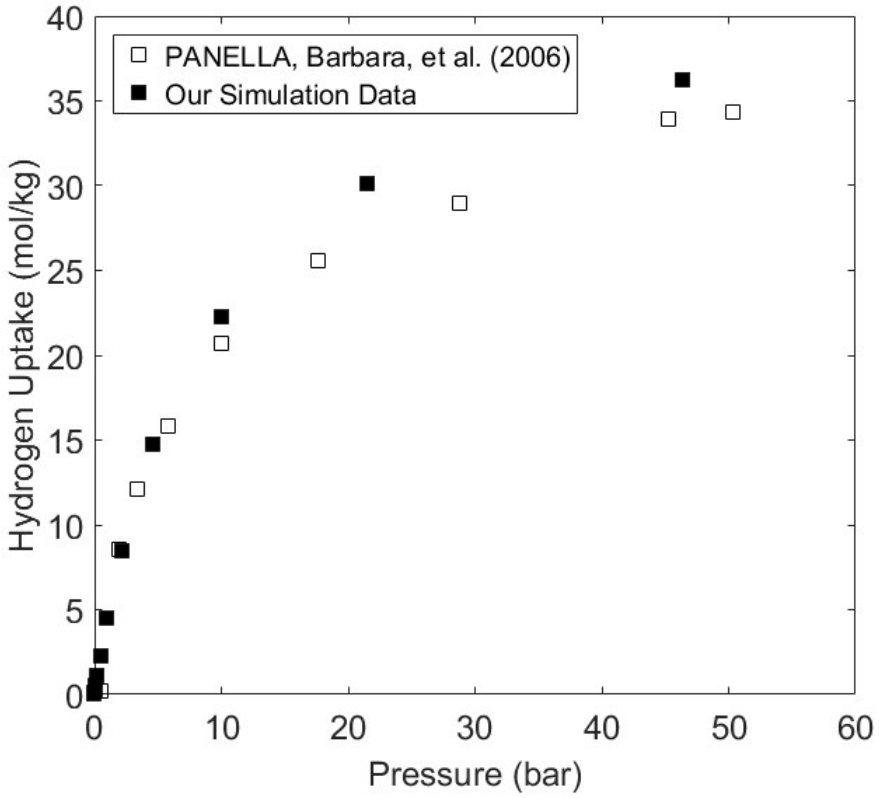

Figure S4-2: Experimental[11] vs simulated H_2 adsorption isotherms in IRMOF-1 at T = 77K.

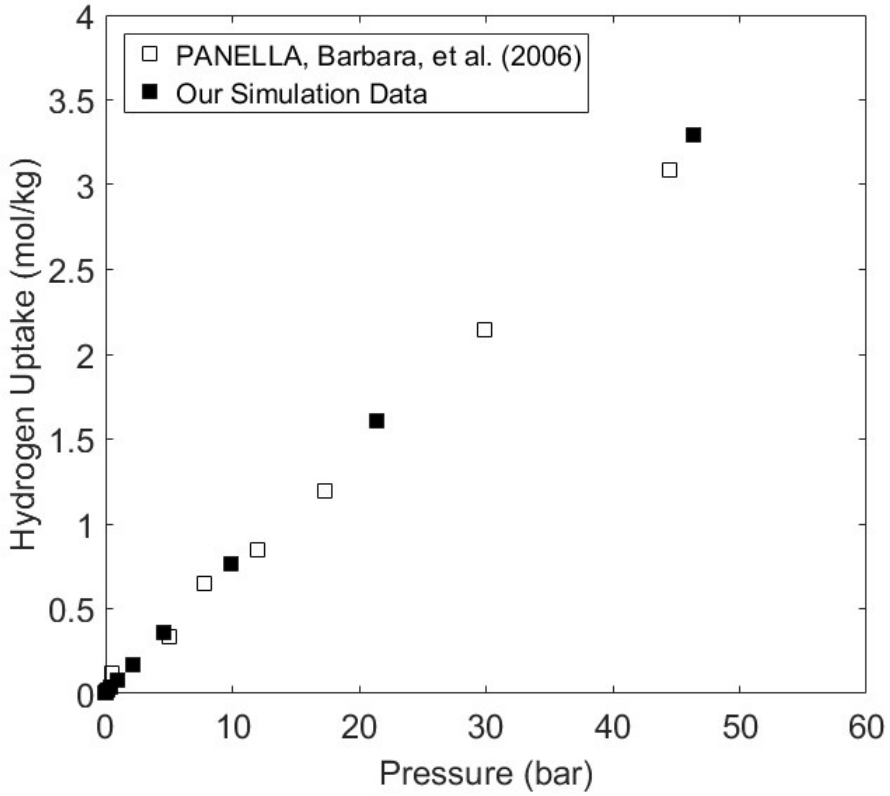

Figure S4-3: Experimental[11] vs simulated H_2 adsorption isotherms in IRMOF-1 at T = 298K.

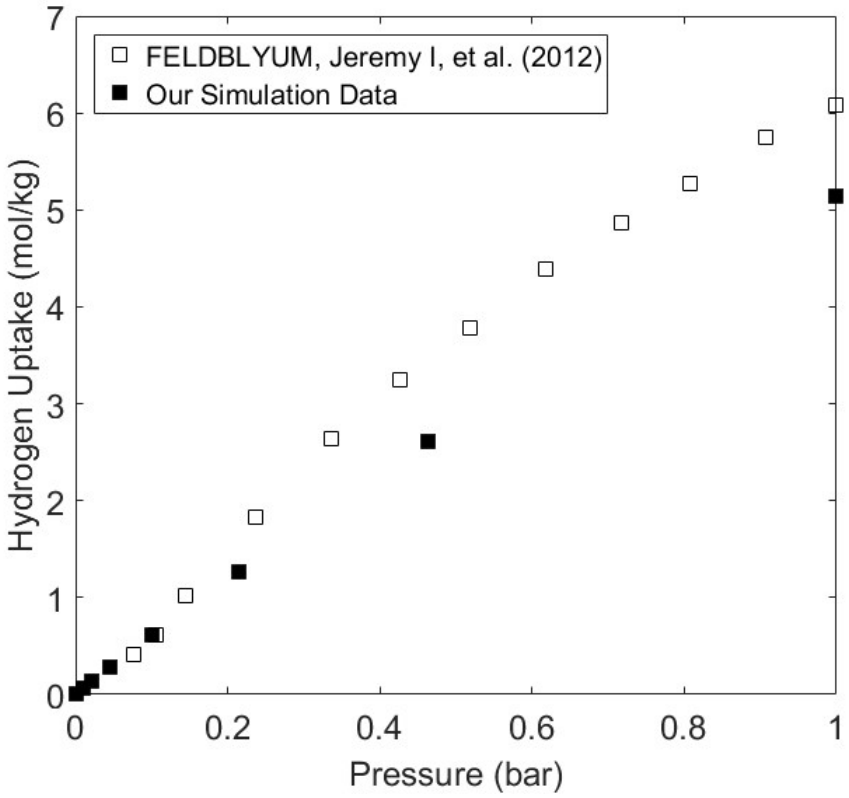

Figure S4-4: Experimental[12] vs simulated H_2 adsorption isotherms in IRMOF-8 at T = 77K.

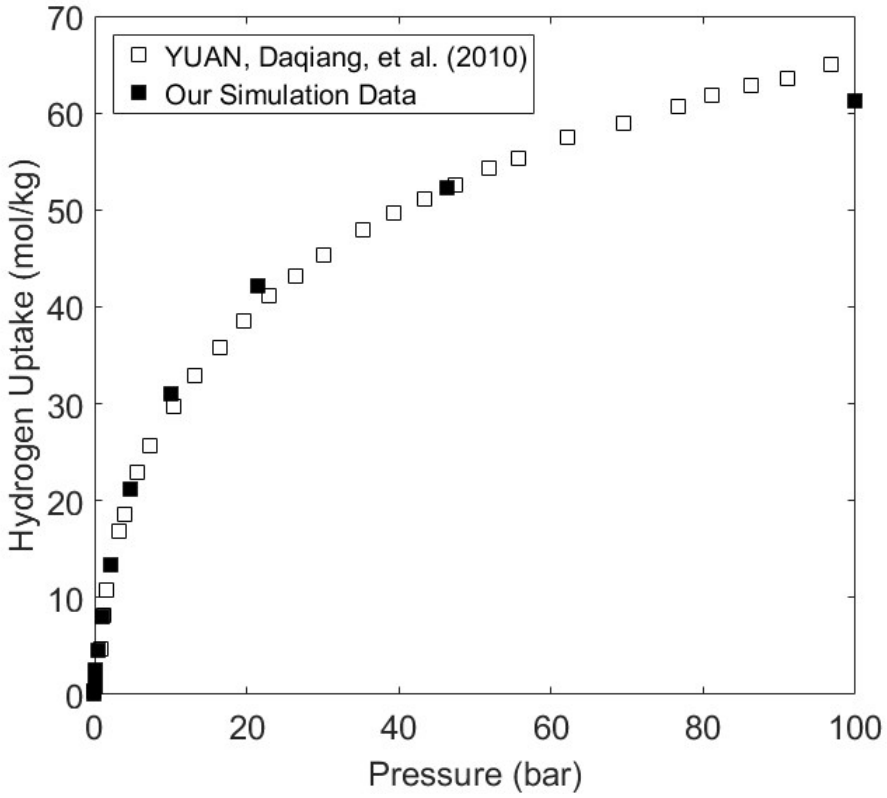

Figure S4-5: Experimental[13] vs simulated H_2 adsorption isotherms in PCN-68 at T = 77K.

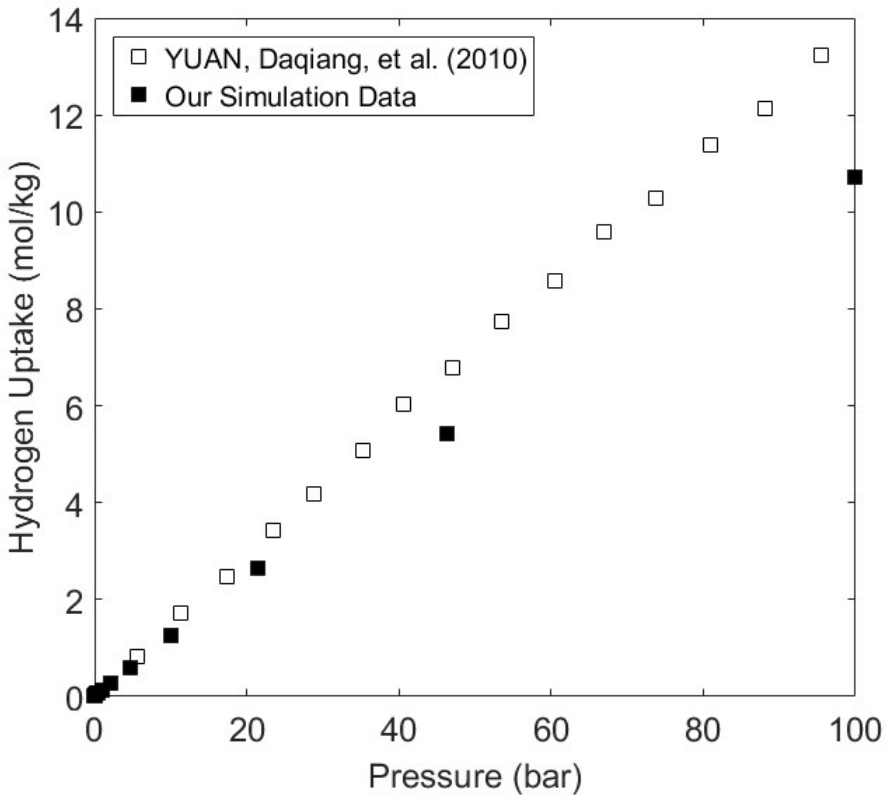

Figure S4-6: Experimental[13] vs simulated H_2 adsorption isotherms in PCN-68 at T = 298K.

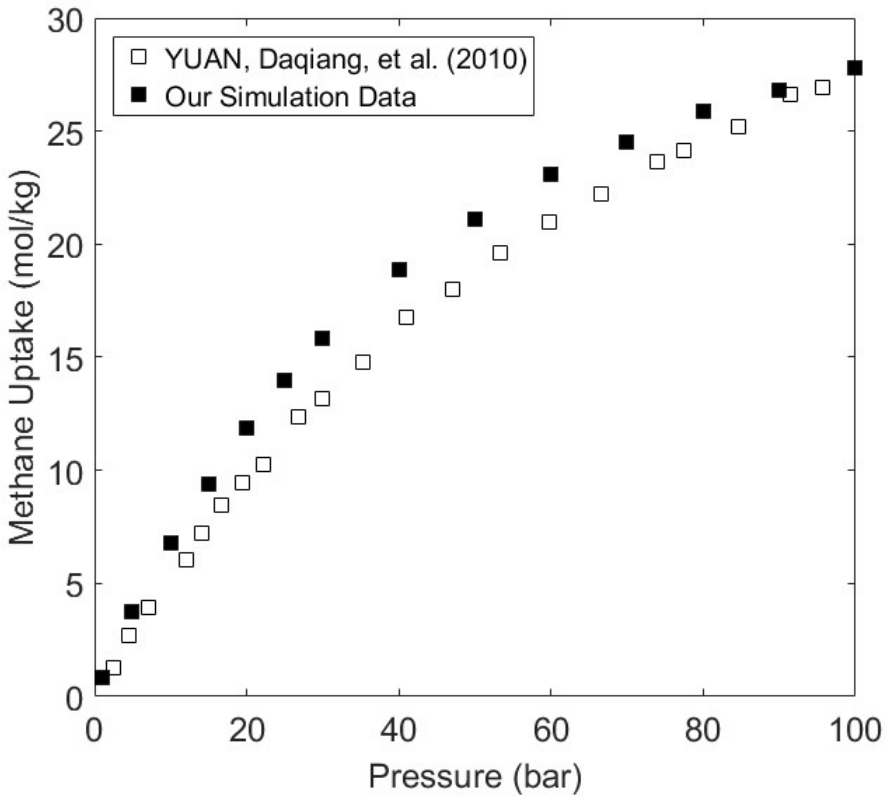

Figure S4-7: Experimental[13] vs simulated CH_4 adsorption isotherms in PCN-68 at T = 298K.

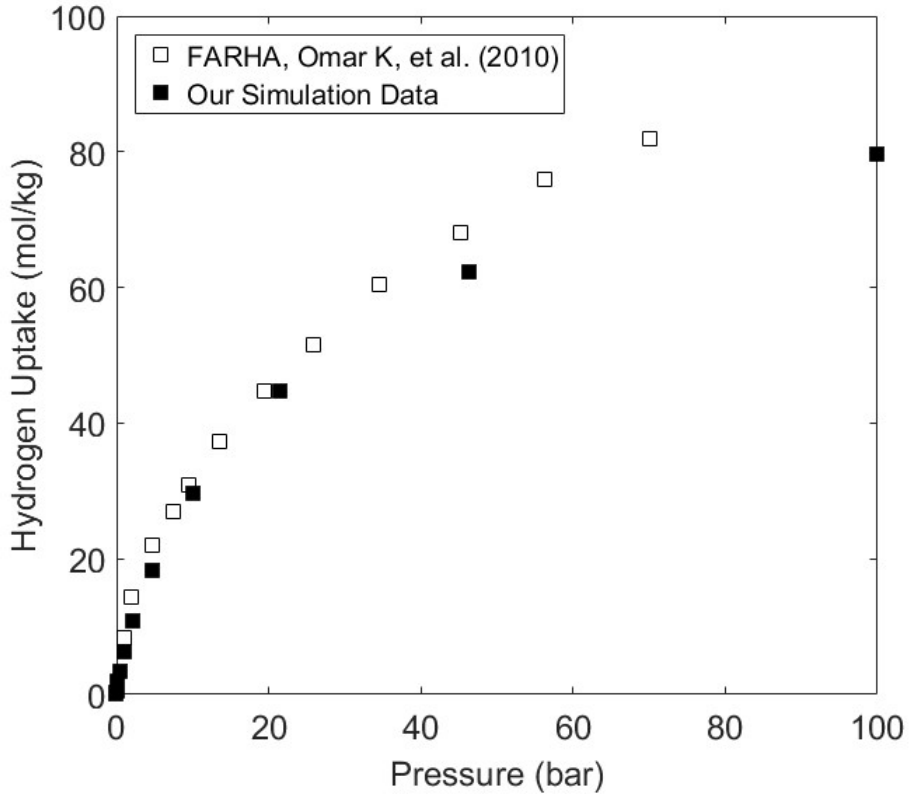

Figure S4-8: Experimental[14] vs simulated H_2 adsorption isotherms in NU-100 (i.e. PCN-610) at T = 298K.

S5 Hydrogen Adsorption Isotherms at T = 298K

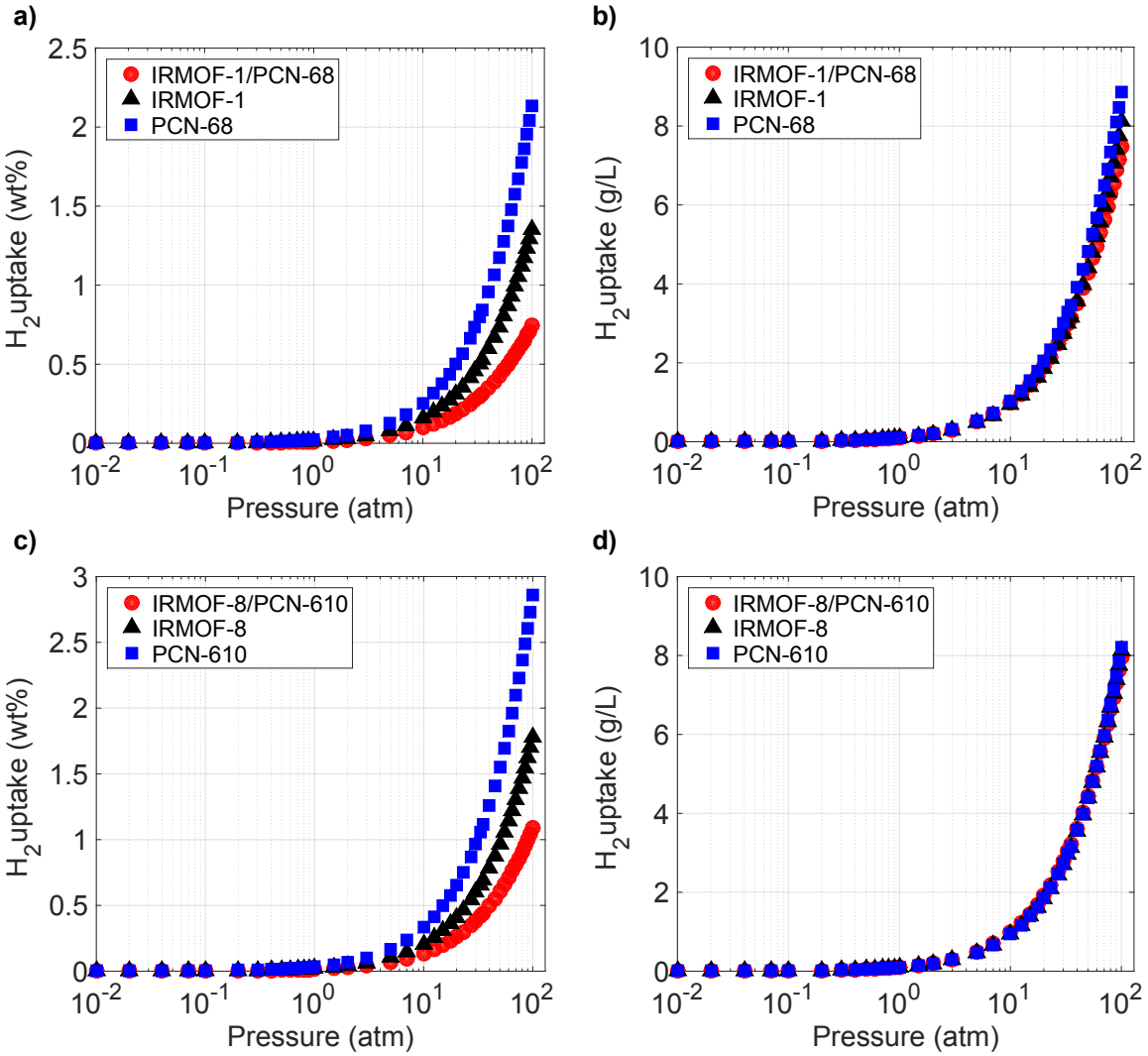

Figure S5(a) Simulated absolute hydrogen uptake (in wt%) for IRMOF-1 (black-triangle), PCN-68 (blue-square), and the hetero-interpenetrated IRMOF-1/PCN-68 (red-circle) at T=298K. (b) Same as (a) but with volumetric uptake. (c) Simulated absolute hydrogen uptake (in wt%) for IRMOF-8 (black-triangle), PCN-610 (blue-square), and the hetero-interpenetrated IRMOF-8/PCN-610 (red-circle) at T=298K. (d) Same as (c) but with volumetric uptake.

1. J. Kim, R. L. Martin, O. Rübel, M. Haranczyk, B. Smit, High-throughput characterization of porous materials using graphics processing units. *Journal of Chemical Theory and Computation* **8**, 1684-1693 (2012).
2. J. Kim, J. M. Rodgers, M. Athènes, B. Smit, Molecular Monte Carlo simulations using graphics processing units: to waste recycle or not? *Journal of Chemical Theory and Computation* **7**, 3208-3222 (2011).
3. A. K. Rappe, C. J. Casewit, K. S. Colwell, W. A. Goddard, W. M. Skiff, UFF, a full periodic table force field for molecular mechanics and molecular dynamics simulations. *Journal of the American Chemical Society* **114**, 10024-10035 (1992).
4. V. Buch, Path integral simulations of mixed para-D_2 and ortho-D_2 clusters: the orientational effects. *The Journal of Chemical Physics* **100**, 7610-7629 (1994).
5. M. G. Martin, J. I. Siepmann, Transferable potentials for phase equilibria. 1. united-atom description of n-alkanes. *The Journal of Physical Chemistry B* **102**, 2569-2577 (1998).
6. L. Firlej, B. Kuchta, Influence of quantum effects on the mechanism of adsorption and phase diagram of rare gases in carbon nanotubes. *Adsorption* **14**, 719-726 (2008).
7. A. V. A. Kumar, H. Jobic, S. K. Bhatia, Quantum effects on adsorption and diffusion of hydrogen and deuterium in microporous materials. *The Journal of Physical Chemistry B* **110**, 16666-16671 (2006).
8. B. Guillot, Y. Guissani, Quantum effects in simulated water by the Feynman–Hibbs approach. *The Journal of Chemical Physics* **108**, 10162-10174 (1998).
9. N. Tchouar, F. Ould-Kaddour, D. Levesque, Computation of the properties of liquid neon, methane, and gas helium at low temperature by the Feynman-Hibbs approach. *The Journal of Chemical Physics* **121**, 7326-7331 (2004).
10. Mason, J. A., Veenstra, M. & Long, J. R. Evaluating metal–organic frameworks for natural gas storage. *Chem. Sci.* **5,** 32–51 (2014).
11. Panella, B., Hirscher, M., Pütter, H. & Müller, U. Hydrogen adsorption in metal-organic frameworks: Cu-MOFs and Zn-MOFs compared. *Adv. Funct. Mater.* **16,** 520–524 (2006).
12. Feldblyum, J. I., Wong-Foy, A. G. & Matzger, A. J. Non-interpenetrated IRMOF-8: synthesis, activation, and gas sorption. *Chem. Commun.* **48,** 9828--9830 (2012).
13. Yuan, D., Zhao, D., Sun, D. & Zhou, H. C. An isoreticular series of metal-organic frameworks with dendritic hexacarboxylate ligands and exceptionally high gas-uptake capacity. *Angew. Chemie - Int. Ed.* **49,** 5357–5361 (2010).
14. Farha, O. K. *et al.* De novo synthesis of a metal-organic framework material featuring ultrahigh surface area and gas storage capacities. *Nat. Chem.* **2,** 944–948 (2010).